MYC Activity Mitigates Response to Rapamycin in Prostate Cancer through Eukaryotic Initiation Factor 4E–Binding Protein 1–Mediated Inhibition of Autophagy

Bala S. Balakumaran,[1] Alessandro Porrello,[1] David S. Hsu,[1,3] Wayne Glover,[1] Adam Foye,[1] Janet Y. Leung,[1,4] Beth A. Sullivan,[1,4] William C. Hahn,[5,7] Massimo Loda,[6] and Phillip G. Febbo[1,2,3,4]

[1]Duke Institute for Genome Sciences and Policy and [2]Duke Comprehensive Cancer Center, Duke University; [3]Division of Medical Oncology, Department of Medicine, and [4]Department of Molecular Genetics and Microbiology, Duke University Medical Center, Durham, North Carolina; Departments of [5]Medical Oncology and [6]Pathology, Dana-Farber Cancer Institute, Boston, Massachusetts; and [7]Broad Institute of Harvard and MIT, Cambridge, Massachusetts

Abstract

Loss of *PTEN* and activation of phosphoinositide 3-kinase are commonly observed in advanced prostate cancer. Inhibition of mammalian target of rapamycin (mTOR), a downstream target of phosphoinositide 3-kinase signaling, results in cell cycle arrest and apoptosis in multiple *in vitro* and *in vivo* models of prostate cancer. However, single-agent use of mTOR inhibition has limited clinical success, and the identification of molecular events mitigating tumor response to mTOR inhibition remains a critical question. Here, using genetically engineered human prostate epithelial cells (PrEC), we show that *MYC*, a frequent target of genetic gain in prostate cancers, abrogates sensitivity to rapamycin by decreasing rapamycin-induced cytostasis and autophagy. Analysis of MYC and the mTOR pathway in human prostate tumors and PrEC showed selective increased expression of eukaryotic initiation factor 4E–binding protein 1 (4EBP1) with gain in *MYC* copy number or forced MYC expression, respectively. We have also found that MYC binds to regulatory regions of the *4EBP1* gene. Suppression of 4EBP1 expression resulted in resensitization of MYC-expressing PrEC to rapamycin and increased autophagy. Taken together, our findings suggest that MYC expression abrogates sensitivity to rapamycin through increased expression of 4EBP1 and reduced autophagy. [Cancer Res 2009;69(19):7803–10]

Introduction

Prostate cancer is the second leading cause of death among men in the United States. Most prostate cancer deaths are due to advanced disease that is refractory to existing treatments. *PTEN* is a tumor suppressor gene that is often lost in advanced prostate cancer, resulting in constitutive activation of the phosphoinositide 3-kinase (PI3K) pathway. PI3K pathway subsequently activates multiple downstream targets, including AKT1 and mammalian target of rapamycin (mTOR), and promotes cell growth and inhibits apoptosis.

The importance of the PI3K-AKT1-mTOR pathway in tumor progression has been elegantly shown *in vivo* using transgenic mouse models. Loss of *PTEN* or expression of activated AKT1 leads to malignant or precancerous lesions in mouse prostate, respectively. Treating transgenic mice expressing myristoylated *AKT1* under a probacin promoter with RAD001 (a rapamycin analogue) for 2 weeks reverses the PIN phenotype, a precancerous lesion of the prostate (1). This dramatic effect of mTOR inhibition reversing the neoplastic phenotype is also observed in transgenic mice with selective prostate knockout of *Pten* (2). Thus, mTOR inhibition with rapamycin or rapamycin analogues is effective in PI3K-driven prostate cancer models.

mTOR signaling is mediated primarily through two multiprotein complexes (TORC1 and TORC2; reviewed in ref. 3). TORC1 includes mTOR, raptor, and mLST8 (also known as GβL; refs. 4–6). When activated, TORC1 phosphorylates two primary downstream effectors, eukaryotic initiation factor 4E–binding protein 1 (4EBP1) and ribosomal protein S6 kinase 1 (S6K1; refs. 7–9). Phosphorylation of 4EBP1 results in the release of eukaryotic initiation factor 4E and increased cap-dependent translation of a set of proteins involved in G_1-S-phase progression including cyclin D and MYC (10, 11). Phosphorylation of S6K1 results in the phosphorylation of the 40S ribosomal protein S6 and the enhancement of translation of mRNAs that possess a 5′-terminal oligopyrimidine tract (12, 13). The TORC2 complex is composed of mTOR, rictor, and mLST8 and has been shown to phosphorylate AKT1 (14) and paxillin (15) among others. Although mTOR is activated in many human cancers, the relative biological importance of TORC1 and TORC2 activity in human cancers remains unknown.

The drug rapamycin binds to a cellular protein FKBP12, and this complex inhibits the TORC1 complex. Despite the dramatic effects observed after treatment of cells in tissue culture and transgenic animals with rapamycin and rapamycin derivatives, limited clinical efficacy of single-agent mTOR inhibition has been observed in advanced prostate cancer. Here, we used genetically engineered prostate epithelial cells and found that MYC expression profoundly reduces sensitivity to rapamycin. Importantly, MYC copy number gain is associated with increased 4EBP1 expression in human prostate tumors, MYC binds to regulatory regions of the 4EBP1 gene, and MYC increases 4EBP1 expression and decreases autophagy. Suppression of 4EBP1 resensitized cells to rapamycin and resulted in less autophagy. In fact, 4EBP1 expression limits autophagy induction by at least two inducers: rapamycin and tunicamycin. Thus, MYC overexpression is associated with increased 4EBP1 expression and decreased autophagy, which may play a role in limiting the clinical effectiveness of single-agent rapamycin or rapamycin analogues.

Note: Supplementary data for this article are available at Cancer Research Online (http://cancerres.aacrjournals.org/).

Requests for reprints: Phillip G. Febbo, Duke Institute for Genome Sciences and Policy, Duke University Medical Center, 2175 CIEMAS Building, Durham, NC 27710. Phone: 919-668-4774; Fax: 919-668-4777; E-mail: phil.febbo@duke.edu.

doi:10.1158/0008-5472.CAN-09-0910

Materials and Methods

Cell lines and medium. Prostate cancer cell lines DU145, LNCaP, and PC3 were obtained from the American Type Culture Collection. Cells were grown in RPMI (Cellgro) with 10% fetal bovine serum. This medium was supplemented with 10 mmol/L HEPES, 1 mmol/L sodium pyruvate, 2 mmol/L L-glutamine, and 1 μg/mL plasmocin. Genetically engineered cell lines including PrEC, LHS, LHSR, LHSR-AR, BH10i-AR, and LHMB-AR were created and propagated as described previously (see Supplementary Table 1 for specific genetic constitution of each cell line; ref. 16). The prostate epithelial cells were incubated at 37°C and 5% CO_2 in PrEGM with defined supplements as recommended (Cambrex).

Retroviral infection. Retroviruses were created as described previously (17) with minor modifications. 293 EBNA packaging cell lines were transfected with each of three plasmids containing (*a*) the Gag and Pol genes, (*b*) the VSV envelope protein gene, and (*c*) a pWZL retroviral vector containing the gene of interest using FuGENE 6 [3:1, volume (μL) to weight (μg) ratio]. Packaging cell lines were transfected twice separated by 24 h; virus was harvested 36 to 48 h following the second transfection. Virus-containing medium was centrifuged at 500 rpm for 5 min at 4°C, filtered (45 μm pore size; μStar), mixed with 10% growth medium and 4 μg/mL polybrene, and placed on cells. The retroviral supernatant was removed 24 h later, cells were cultured for another 24 h in normal growth medium, and selective medium containing the appropriate agent (blasticidin or puromycin) was added. Lentiviral infections were done following a similar protocol to the retroviral infections. Lentiviral packaging vectors (pLKO system) were obtained from Addgene (Trono Laboratory). short hairpin RNA (shRNA) construct against 4EBP1 in lentiviral vector was from the RNAi Consortium (Broad Institute).

Plasmids and bacteria. All plasmids were propagated in DH5α *Escherichia coli* bacteria (Invitrogen) in Luria-Bertani growth medium (Fisher Scientific) and grown at 37°C. The vector backbone pWZL was obtained as pWZL-MYC from Addgene (18). The enhanced green fluorescent protein insert was from pEGFP-C1 (BD biosciences). The shRNA construct against MYC, sh3.1, was a gift from Joseph Nevins (Duke University) and is in pRETROSUPER (19).

Drug sensitivity assay. Rapamycin (Sigma-Aldrich) and a PI3K inhibitor (BEZ235; Novartis) were used in prostate cancer cell lines (DU145, PC3, and LNCaP) as well as in genetically engineered cell lines to determine the sensitivity of the cells to the two drugs using a propidium iodide–based cell cytotoxicity assay (20). Cells were plated at a density of 5,000 per well in 100 μL tissue culture medium. Serial dilutions of the drug at varying concentrations were added in a volume of 100 μL the next day, one set of plates is taken out at this point as a time 0 control, and plates are incubated for 4 to 5 days after which they are removed from the incubator and frozen at −80°C. At least 12 h after being frozen, the plates were thawed, 50 μL (stock 200 μg/mL) of propidium iodide were added to each well, and plates were incubated for 1 h in dark. Fluorescent readings were measured with a FLUOstar OPTIMA (BMG Labtech) with excitation at 530 nm and emission at 590 nm wavelengths. Proliferation was normalized to the no drug control and plotted against increasing drug concentration using Microsoft Excel software. Inhibitory concentrations were obtained using GraphPad to obtain a nonlinear regression curve fit to calculate the EC_{50} (Prism Software).

Protein isolation and Western blotting. Cells were solubilized in radioimmunoprecipitation assay lysis buffer (supplemented with mini cocktail EDTA free proteinase inhibitors; Roche). Adherent cells were washed in ice-cold PBS twice and harvested using a cell scraper. Cells were resuspended in radioimmunoprecipitation assay lysis buffer (supplemented with mini cocktail EDTA free proteinase inhibitors; Roche). When rapamycin and BEZ235 were used to investigate the effect on protein phosphorylation, cells were starved for 48 h in 0.2% serum-containing medium (or PrGEM that has only 1/50th of the recommended supplements) and released in medium containing 10% serum for 30 min before protein isolation. Protein lysates (25 μg/sample) were separated on precast gradient gels (Bio-Rad) by electrophoresis and transferred to a nylon membrane (Immobilon-P). The membrane was blocked in 5% nonfat dry milk for 1 h and hybridized to primary antibodies in TBS-Tween 20 overnight at 4°C. Membrane was washed in TBS-Tween 20 for 5 min three times and incubated in secondary antibody anti-mouse or anti-rabbit linked to horseradish peroxidase (1:2,000) for 1 h. Following five washes of 5 min each, membrane was processed using Enhanced Chemiluminescence Western Blotting Reagents (Amersham, GE Healthcare) and exposed to film (Hyblot CL, Denville Scientific). The following primary antibodies were purchased from Cell Signaling Technology: LC3B, pS6, total S6, pAKT1 (Ser^{473}), total AKT1, p4EBP1, total 4EBP1, eIF4E, and caspase-3. The antibodies against c-MYC and actin were from Santa Cruz Biotechnology and the antibody against poly(ADP-ribose) polymerase was from Upstate Biotech. The secondary antibodies were either horseradish peroxidase–linked anti-rabbit or anti-mouse both from Cell Signaling Technology.

Cell cycle analysis. Cells were grown at low density on plates and rapamycin was added at different concentrations and exposed for different periods. When harvesting cells, culture medium was saved and spun to preserve floating and loosely attached cells. Attached cells were detached using trypsin and all cells for each treatment were collected in a 1.5 mL microcentrifuge tube and spun at 2,000 rpm for 2 min. Cells were washed in PBS, fixed in 70% ethanol, and resuspending in ice-cold Nuclear Isolation Medium (0.5% bovine serum albumin and 0.1% NP-40 in PBS) containing 5 μg/mL propidium iodide and 100 μg/mL DNase-free RNase. Cell cycle phases in 5,000 to 10,000 cells were determined by flow cytometry at the Duke Flow Cytometry Facility.

RNA expression and tissue microarrays. Deidentified local prostate cancer specimens were analyzed under an institutional review board–approved protocol (Duke institutional review board 6679-04EX). PrEC cell lines and tumor specimens were processed for hybridization to Oligonucleotide microarrays (Affymetrix U133A) using standard methods (17, 21). Gene expression was determined from the CEL files using RMA with background correction and quantile normalization (22, 23). Expression of MYC, mTOR, 4EBP1, S6, S6K, and AKT was determined using gene-specific probes on the U133A microarray.

Formalin-fixed, paraffin-embedded tissue for a subset of the samples for which frozen tissue was available for microarray analysis was used to create tissue microarrays. MYC copy number gain was determined using fluorescent *in situ* hybridization as described previously (24).

Nonparametric tests were used to determine statistical significance of differences between cell lines (Mann-Whitney) or correlation between the expression of specific genes (Spearman's rank statistic).

Chromatin immunoprecipitation assay. Chromatin immunoprecipitation assay was done as described previously (19). Briefly, 10% formaldehyde solution was added to cells for 15 min to crosslink DNA-protein complexes. Isolated nuclear chromatin extracts were sonicated and incubated overnight at 4°C with antibodies from Santa Cruz Biotechnology with either 5 μg anti-c-MYC or 2.5 μg normal rabbit IgG. This was followed by incubation with 20 μL protein A agarose beads (Roche) for 3 to 4 h at 4°C. After extensive washing, DNA fragments were harvested by de-cross-linking the immunoprecipitates. Real-time PCR using SYBR Green Master Mix (Qiagen) and the ABI PRISM 7900 Sequence Detection System was used for quantitative analysis of the recovered DNA fragments from chromatin immunoprecipitation including regions of *4EBP1, ALB*, and *ODC1* (see Supplementary Table S2 for primer sequences). Relative occupancy of the MYC transcription factor at the different E-boxes were estimated by comparing its occupancy at the albumin promoter following methods described previously (25). The chromatin immunoprecipitation assays were done at least three times for each cell line.

Autophagy assays. Cells were grown in 10 cm plates in the presence of absence of rapamycin or tunicamycin for 24 h and harvested for analysis. For Western blots, cell lysates were separated using PAGE (as described above) and hybridized to an antibody for LC3B type II (Cell Signaling Technology) at 1:1,000 to detect autophagosome formation. For flow cytometry, cells were exposed to 1 μg/mL acridine orange (Sigma-Aldrich) for 20 min, trypsinized, and resuspended in growth medium. Approximately 20,000 cells were analyzed using the PerCP-Cy5.5-A channel with a BD FACS Canto II (BD Biosciences) flow cytometer. For fluorescent microscopy, cells were grown on tissue culture–treated chamber slides (BD Falcon) and

exposed to rapamycin or tunicamycin for 24 h. The cells were briefly exposed to 1 μg/mL acridine orange (Sigma-Aldrich) for 20 min and examined under a microscope without fixation. All images were acquired using an inverted Olympus IX71 microscope and Photometrics Cool Snap HQ camera connected to a Deltavision RT Restoration Imaging System (Applied Precision). Images were acquired using the ×20 Uplan SApo objective (0.75 NA) and the Deltavision SoftWoRx Resolve 3D capture program and collected as a stack of 0.2 to 0.5 μm increments in the *z* axis (15-35 sections). Images were deconvolved using the conservative algorithm with 5 to 10 iterations. Deconvolved images were saved as separate *z*-sections or viewed as stacked (collapsed) images using the Quick Projection option. Images were then imported to Adobe Photoshop for presentation.

Results

Genetic determinants of prostate cell sensitivity to rapamycin. Prior studies (26) have shown that the *PTEN* status of established prostate cancer cell lines affects sensitivity to rapamycin; *PTEN* wild-type cells (DU145) are less sensitive than *PTEN*-null cell lines (PC3 and LNCaP; Supplementary Fig. S1*A*). However, the marked aneuploidy present in these established cancer cell lines (27–29) precludes refined analysis regarding specific interactions between genetic events and sensitivity to rapamycin. Therefore, genetically engineered immortalized and tumorigenic human prostate epithelial cells (PrEC; ref. 16) were tested for rapamycin sensitivity. In these cell lines, neither activated H-Ras nor the androgen receptor (AR) significantly altered PrEC sensitivity to rapamycin (Fig. 1*A* and *B*; Supplementary Fig. S1*B*). In contrast, the expression of MYC resulted in marked resistance to rapamycin (Fig. 1*A* and *B*). In multiple experiments, the EC_{50} for rapamycin was the same for cell lines with differential expression of RAS (LHS EC_{50} 0.18 ± 0.11 nmol/L versus LHSR EC_{50} 0.21 ± 0.16 nmol/L; mean ± SD) or AR (LHSR EC_{50} 0.21 ± 0.16 nmol/L versus LHSR-AR EC_{50} 0.16 ± 0.14 nmol/L), whereas there was ∼10-fold difference in the EC_{50} between cell lines with differential expression of MYC (BH10i-AR EC_{50} 0.23 ± 0.060 nmol/L versus LHMB-AR EC_{50} 2.13 ± 1.963 nmol/L; P = 0.0286, Mann-Whitney exact). Although MYC is known to be an important downstream target of mTOR-mediated regulation of cap-dependent translation (11), the ability of MYC to abrogate sensitivity to rapamycin has not been previously described.

Altering MYC levels in established prostate cancer cell lines mimics the effects seen in the PrEC. MYC expression also affects rapamycin sensitivity in established prostate cell lines (PC3, DU145, and LNCaP). Consistent with our findings in PrEC, overexpression of MYC resulted in decreased sensitivity to rapamycin in LNCaP and DU145 (Fig. 2*A* and *B*). Increased expression of MYC in PC3 had minimal effect on rapamycin sensitivity and we note that baseline expression of MYC in PC3 is higher than DU145 and LNCaP (Fig. 2*A*). RNA interference–mediated suppression of MYC increased rapamycin sensitivity in all three cell lines tested (Fig. 2*C* and *D*). Altering MYC in the established cell lines affected the growth kinetics of each cell line independent of rapamycin exposure. To ensure that MYC activity rather than a change in cell growth altered rapamycin sensitivity, we tested a range of serum deprivation conditions to identify a concentration of serum that resulted in an equivalent reduction in cell growth as seen with MYC knockdown. PC3 cells growing in 2.5% serum had an equivalent reduction in cell growth as seen with MYC knockdown (∼70%) but were not more sensitive to rapamycin (data not shown). Overall, altering MYC expression in established prostate cancer cell lines consistently altered sensitivity to rapamycin albeit less dramatically as in the genetically engineered PrEC cell lines.

MYC alters rapamycin-induced cytostasis and autophagy. In previous reports, mTOR inhibition with rapamycin has been found to cause cytostasis (1), apoptosis (1), and/or autophagy (30). In the PrEC cell lines, the effect of MYC appears to be primarily through decreased rapamycin-induced cytostasis and autophagy rather than apoptosis. In the BH10i-AR cells, rapamycin treatment results in a marked cytostasis with a decrease in the percentage of cells in the S and G_2 phases of the cell cycle (Fig. 3*A*). Expression of MYC abrogates the rapamycin-induced cytostasis. The effect of MYC was not due to apoptosis as rapamycin failed to induce apoptosis in either BH10i-AR or LHMB-AR cell lines as detected by proteolytic cleavage of caspase-3 (Supplementary Fig. S2*A*) or poly(ADP-ribose) polymerase (Supplementary Fig. S2*B*), although MYC

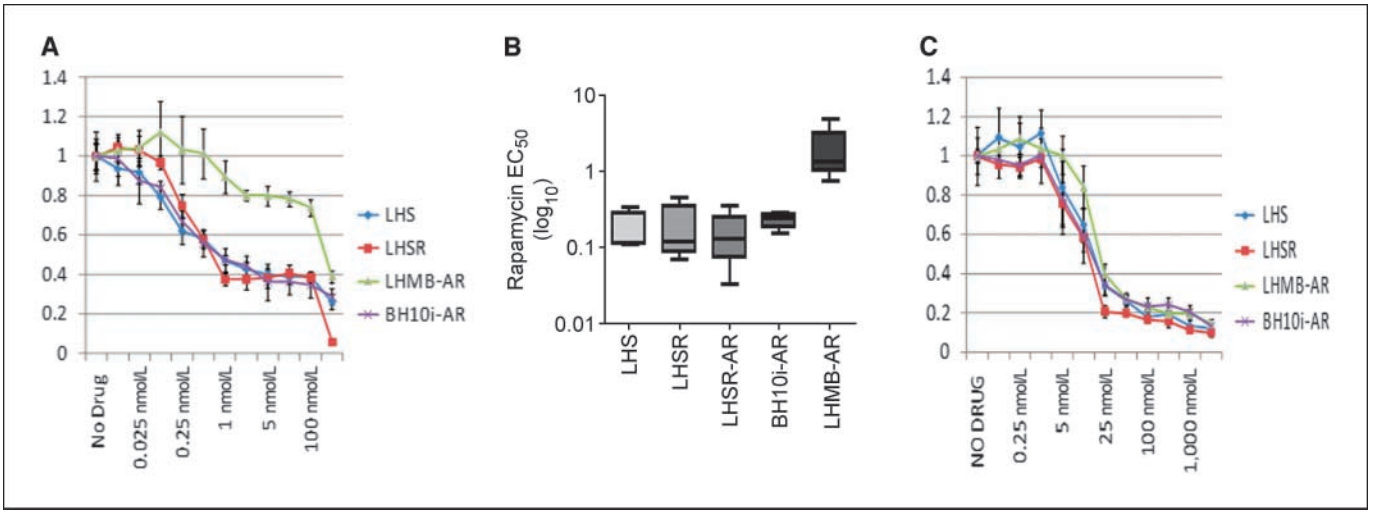

Figure 1. Overexpression of the oncogene c-*MYC* in prostate cell lines confers resistance to the mTOR inhibitor rapamycin but not to a PI3K inhibitor. *A,* normalized cell cytotoxicity (*Y axis*) for four genetically engineered prostate epithelial cell lines (PrEC) exposed to increasing concentrations of rapamycin (*X axis*). Absorbance values are normalized to the no drug control individually for each cell line. *B,* EC_{50} (rapamycin) of the PrEC plotted on a $\log_{10}$ scale. *C,* sensitivity of PrEC cell lines to a PI3K inhibitor. Cytotoxicity is normalized as in *A*.

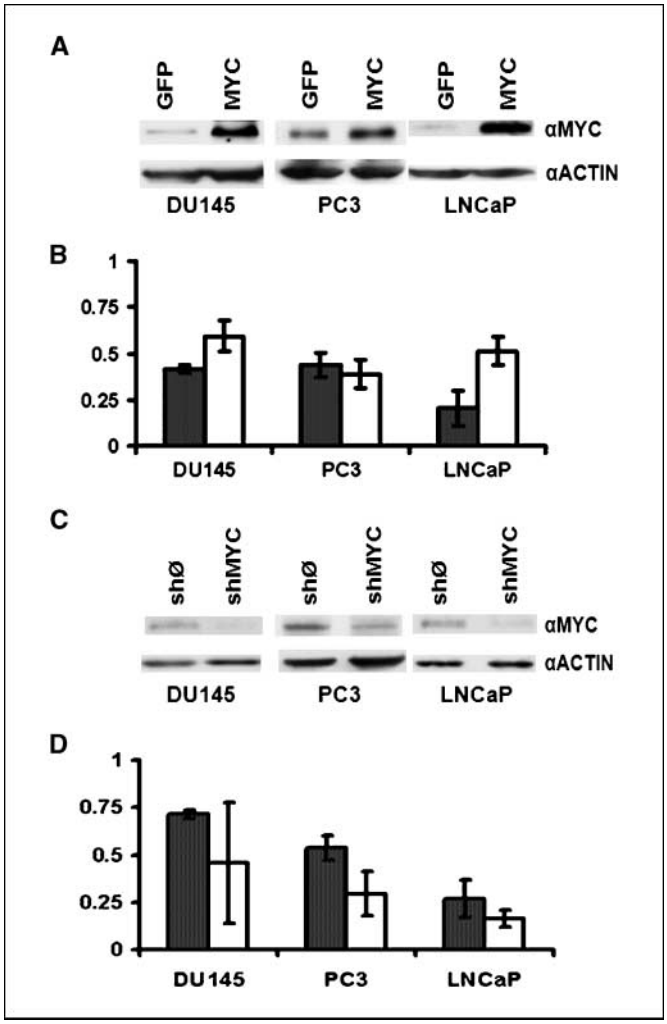

Figure 2. MYC affects response to rapamycin in established prostate cancer cell lines. *A,* Western blots for MYC (*αMYC*) and actin *(αACTIN*) of antibiotic-resistant polyclonal cell lines DU145, PC3, and LNCaP after infection with a retrovirus construct containing GFP or MYC. *B,* relative cell number after 4 d of growth in medium containing 5 nmol/L rapamycin for DU145, PC3, and LNCaP cells expressing either GFP (*gray columns*) or MYC (*white columns*). Relative cell number is determined by the emission at 590 nm after staining with propidium iodide normalized to cells grown for 4 d without rapamycin. *C,* Western blot for MYC and actin of stable, polyclonal cell lines DU145, PC3, and LNCaP after infection with a retrovirus containing a scrambled shRNA or sh3.1, which targets MYC. *D,* relative cell number after 4 d of growth in medium containing 5 nmol/L rapamycin for DU145, PC3, and LNCaP cells infected with either a scrambled shRNA construct (*shØ*; *gray columns*) or sh3.1 targeting MYC (*shMYC*; *white columns*). Relative cell number is determined as above.

expression did decrease the sub-G_1 population of cells (the "M1" gate in Fig. 3*A*) with or without rapamycin. The specificity of the observed effect of MYC on rapamycin sensitivity is supported by a failure of activated H-RAS in the PrEC to have a similar decrease in rapamycin-induced cytostasis (Supplementary Fig. S2*C*).

Cells detected to be in G_1-G_0 may simply be in a state of dormancy (e.g., G_0) but they can exhibit alternative behaviors such as autophagy. In the PrEC, MYC expression decreased autophagy as measured by acridine orange staining, flow cytometry, and LC3B Western blot (Fig. 3*B*) and limited the increase in autophagy following treatment with rapamycin (Fig. 3*B-D*). Coincident exposure to bafilomycin A1 decreased baseline autophagy and eliminated rapamycin-induced autophagy. MYC expression also limited autophagy caused by tunicamycin, a frequently used agent that reliably causes autophagy through inhibition of GlcNAc phosphotransferase and inhibition of glycoprotein synthesis, a mTOR-independent process. However, we did not see a difference in autophagy induction between the PrEC cell lines with and without MYC expression using Earle's BSS, *N*-acetylsphingosine, or lithium chloride (Supplementary Fig. S2*D*).

Analysis of the expression of downstream mTOR components *in vitro* and *in vivo* in genetically engineered prostate epithelial cells and prostate tumors. After establishing an association between MYC activity and rapamycin sensitivity, we sought to investigate how MYC, a transcription factor, may affect the mTOR signaling cascade. To identify mTOR target proteins that may have altered expression due to MYC, we analyzed transcriptional microarray data derived from the PrEC cell lines and a set of prostate tumors for which we have microarray data and tissue microarrays.

First, we used gene expression profiles from the PrEC to determine if mTOR, S6K, 4EBP1, or AKT1 were differentially expressed in the presence or absence of MYC. In PrEC lines of different genetic constitutions, 4EBP1 was specifically overexpressed in cells expressing MYC and not altered by any other genetic manipulation (Fig. 4*A*). MYC, however, did not affect the expression of S6K, mTOR, or AKT1.

Next, we tested if genetic gain of *MYC* in prostate cancer tumors was associated with increased expression of mTOR and/or target proteins. Using a set of 50 tumors for which both tissue microarrays and expression data were available, MYC copy number was definitively established in 21 specimens by fluorescent *in situ* hybridization (Fig. 4*B, left*) and transcriptional microarray analysis was used to determine expression of specific mTOR targets. Here, although the number of samples with gain in MYC copy number was relatively small (n = 6), 4EBP1 had increased expression in prostate tumors with increased *MYC* copy number compared with samples that were diploid for *MYC* (P = 0.0091; Fig. 4*B, right*). In addition, in a larger number of prostate cancer samples, MYC RNA expression significantly correlated with 4EBP expression (Spearman r = 0.453; P = 0.0391), whereas there was no correlation between MYC and mTOR (Spearman r = -0.229; P = 0.316; Supplementary Fig. S3*A*).

Thus, in genetically engineered cell lines and localized prostate cancer specimens, there is a consistent correlation between MYC and increased expression of 4EBP1 that was not apparent with other target proteins of mTOR.

MYC binds to E-box sequence adjacent to *4EBP1* gene. Given the correlation between MYC copy number gain and 4EBP1 expression, we performed chromatin immunoprecipitation to determine if MYC binds to regulatory regions of the 4EBP1 gene. One E-box sequence was identified immediately upstream of the 4EBP1 transcriptional start site and two additional E-box sequences were identified within the first intron of 4EBP1 (see schema in Fig. 4*C*). In LHMB-AR, there was strong relative occupancy of E-boxes 1 and 2 when compared with an unrelated albumin promoter region but no occupancy of E-box 3 (Fig. 4*C*). MYC occupancy of E-boxes 1 and 2 was greater in LHMB-AR than MYC occupancy of an E-box adjacent to the ornithine decarboxylase gene, which is a well-characterized direct MYC target (31). MYC also occupied E-box 1, E-box 2, and the E-box adjacent to ornithine decarboxylase in the BH10i-AR cell line but at much lower relative occupancy (Supplementary Fig. S3*B*). Binding of MYC to E-boxes 1 and 2 was also observed in the established prostate cancer cell line PC3, although relative MYC occupancy was

somewhat lower than at the ornithine decarboxylase gene (Fig. 4*C*). Thus, MYC likely increases 4EBP1 expression through direct transcriptional regulation.

MYC expression increases expression of 4EBP1 protein. We next investigated MYC-induced changes in the protein expression and phosphorylation status of mTOR target proteins in the genetically engineered prostate cell system. When the expression and phosphorylation of S6, 4EBP1, and AKT1 were assessed, we found a marked increase in total 4EBP and p4EBP in the LHMB-AR cells, whereas total S6 and pS6 levels did not change and AKT1 was only modestly increased (Fig. 4*D*). In the PrEC, rapamycin significantly decreases phosphorylation of S6 and increases phosphorylation of AKT1 but had limited effect on 4EBP phosphorylation in MYC-expressing cells. This pattern appears to be specific to mTOR inhibition with rapamycin, as inhibition of both PI3K and mTOR with BEZ235 inhibited phosphorylation of all three proteins (Supplementary Fig. S4*A* and *B*). The increase in protein expression of 4EBP1 with MYC overexpression is also observed in PC3 cells, an established prostate cancer cell line (Supplementary Fig. S4*C*). In addition, levels of eIF4E were consistent despite increased MYC expression and increased 4EBP1 expression (Supplementary Fig. S4*D*), suggesting that along with increased total levels of 4EBP1 there was also an increase in the ratio of 4EBP1 to eIF4E.

4EBP1 suppression resensitizes MYC-expressing PrEC to rapamycin and increases autophagy. The strong association between MYC and 4EBP1 expression suggests that MYC may confer increased resistance to rapamycin through increased 4EBP1 expression. Although 4EBP1 does not coimmunoprecipitate with the TORC1 complex in the PrEC and established prostate cancer cell lines (data not shown), we remained interested in determining if decreasing 4EBP1 would alter rapamycin sensitivity in PrEC with high MYC expression. To test this, 4EBP1 was targeted with a shRNA in LHMB-AR PrEC. Although suppression of 4EBP1 had no effect on LHMB-AR cell growth, the cells became significantly more sensitive to rapamycin (Fig. 5*A*).

As MYC decreased autophagy and limited the increase in autophagy resulting from rapamycin treatment, we determined if

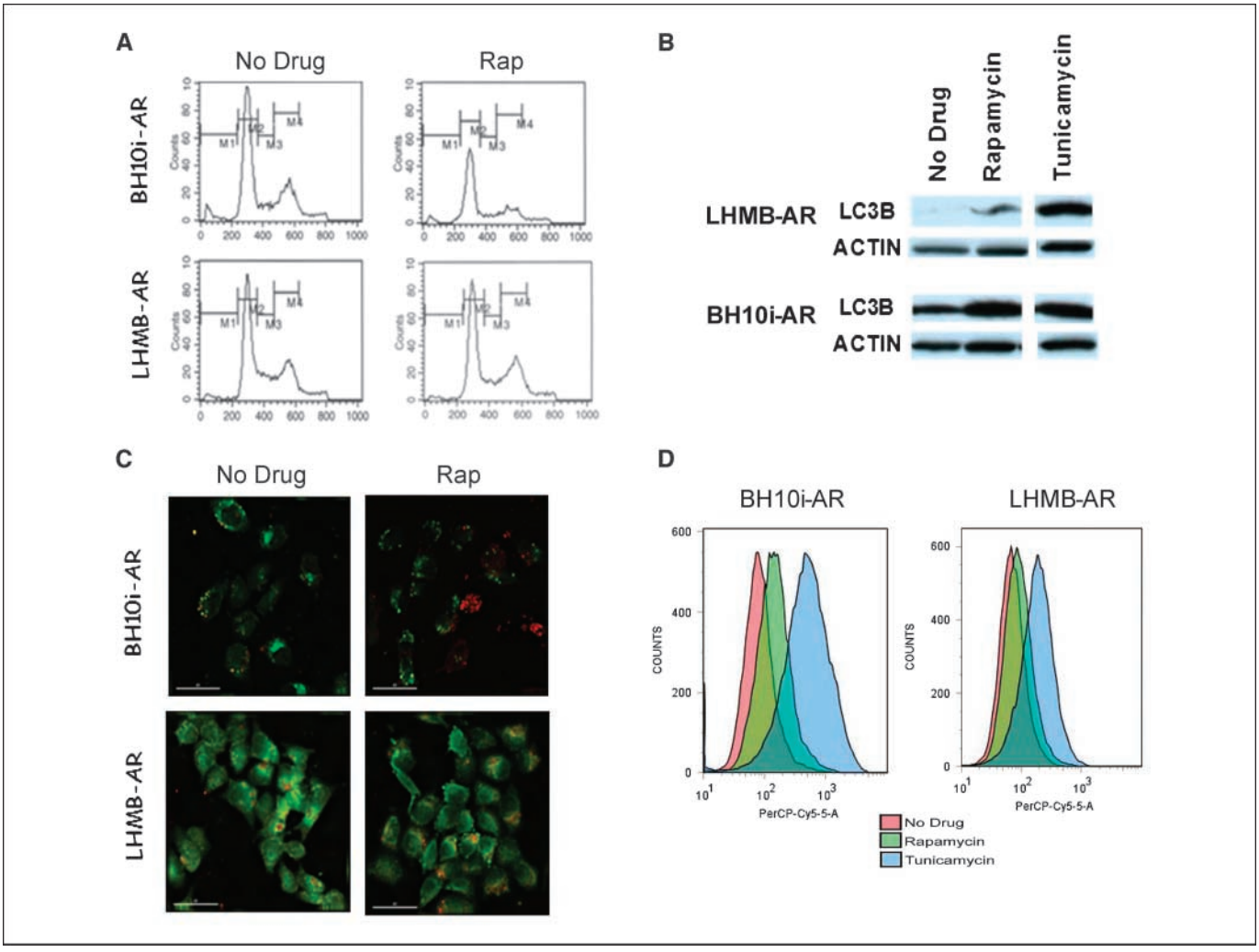

Figure 3. Rapamycin sensitivity is mediated by alteration in cell cycle progression and autophagy. *A,* LHMB-AR and BH10i-AR cells are grown in the presence or absence of rapamycin (*Rap*) for 24 h and cell cycle analysis was done by flow cytometry (described in Materials and Methods). *B,* LC3B analysis by Western blotting for autophagy after exposure for 24 h to 1 μmol/L rapamycin or 2.5 μmol/L tunicamycin. *C,* fluorescent images of cells grown for 24 h at 20 nmol/L rapamycin and control cells without rapamycin (as described in Materials and Methods). Autophagosomes are the red vesicles in the cytoplasmic region. *Bar,* 40 μm. *D,* autophagy analyzed using flow cytometry. Cells were grown in the presence of 20 nmol/L rapamycin, 2.5 μmol/L tunicamycin, or no drug for 48 h and stained with acridine orange. Each treated group for either cell line is statistically different from the untreated group ($P < 0.0001$, Mann-Whitney test).

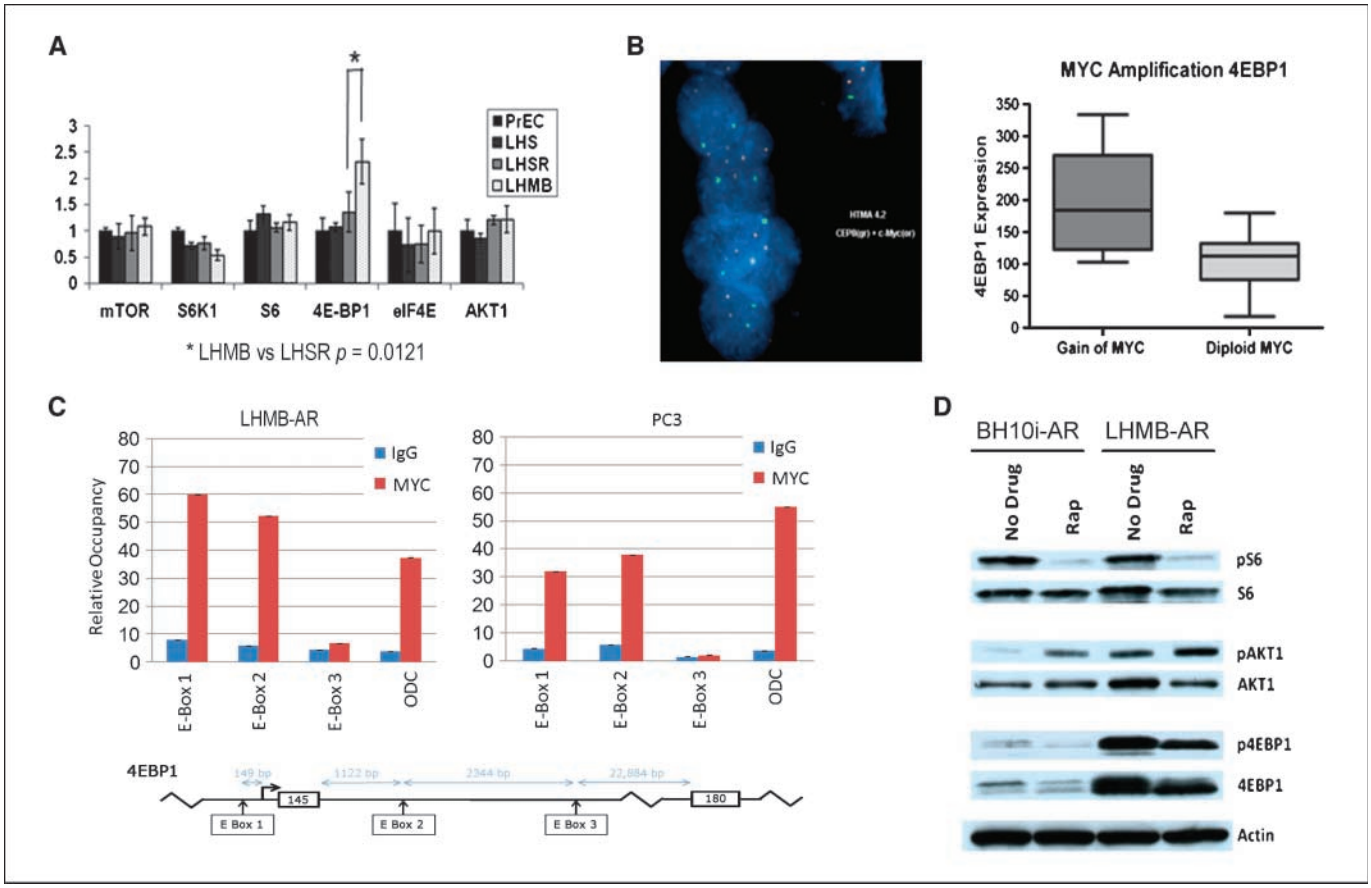

Figure 4. MYC expression leads to increased 4EBP1 in cell lines and tumor samples. *A,* RNA expression levels of the different components of the mTOR pathway in the genetically engineered prostate epithelial cell lines. RNA levels are normalized to that expressed in the unmodified PrEC. *B,* MYC amplification in prostate tumors from patients detected by fluorescent *in situ* hybridization. Box plot of 4EBP1 expression for samples with gain of c-MYC ($n = 6$) versus those that are diploid ($n = 15$). In representative image of cells with c-MYC gain, c-MYC probe is in red and CEN8 probe in green. *C,* results of chromatin immunoprecipitation in LHMB-AR and PC3 cell lines using nonspecific rabbit polyclonal antibody (IgG; *blue columns*) or a MYC-specific antibody (MYC; *red columns*). Relative occupancy (*Y axis*) plotted for three regions containing an E-box adjacent to the 4EBP1 transcriptional start site (E-boxes 1-3) and ornithine decarboxylase (*ODC*). Locations of each E-box depicted in schematic of 4EBP1 gene. *D,* protein expression and phosphorylation status of mTOR effector proteins in prostate epithelial cells expressing hTERT, large T, activated p110, and AR (*BH10i-AR*) and this same cell line with the additional expression of MYC (*LHMB-AR*). Cells were grown to log phase in normal medium and incubated for 48 h in medium equivalent to serum-starved conditions and then transferred to normal medium for 30 min with or without rapamycin.

knockdown of 4EBP1 affected autophagy. Importantly, decreased 4EBP1 expression resulted in increased baseline levels of autophagy based on lipidation of LC3B and acridine orange fluorescence (Fig. 5*B-D*). Indeed, whereas LHMB-AR cells expressing a lentivirus expressing a scrambled shRNA construct had baseline levels of autophagy similar to that of uninfected LHMB-AR, the LHMB-AR cells in which 4EBP1 expression was suppressed exhibited increased baseline levels of autophagy. Importantly, suppression of 4EBP1 also increased rapamycin- and tunicamycin-induced autophagy (Fig. 5*D*). Thus, 4EBP1 expression appears to have significant effect on autophagy, both baseline levels and selected inducers of autophagy including rapamycin.

Discussion

The PI3K pathway remains a promising target for therapeutic intervention in prostate cancer given the high frequency of *PTEN* loss. Indeed, recent findings from comprehensive cancer genome sequencing projects suggest that the PI3K pathway is frequently activated in breast cancer (32), pancreatic cancer (33), and glioblastoma (34). Although mTOR inhibitors have shown outstanding preclinical activity in prostate cancer models dependent on activation of the PI3K pathway, the limited clinical activity of mTOR inhibition observed in prostate cancer has been disappointing. Although it has been shown that feedback loops through insulin-like growth factor receptor-I and mitogen-activated kinases play a role in resistance to mTOR inhibitors, our work suggests that expression of *MYC*, a target of gain or amplification in 20% to 30% of advanced prostate cancer (35–37), may also account for the limited activity of mTOR inhibition in prostate cancer.

Although MYC has a myriad of transcriptional targets and profound effects on cell biology, our work identifies *4EBP1* as a novel target of MYC through which MYC activity affects the response to rapamycin. 4EBP1 is believed to primarily control cap-dependent translation by binding and inactivating eIF4E; phosphorylation of 4EBP1 results in the release of eIF4E and subsequent activation of the eIF4G scaffolding protein (38). Thus, it is unclear how increased expression of p4EBP1 results in decreased rapamycin sensitivity. Recent work suggests that 4EBP1 may also have a positive effect as p4EBP1 can bind to and stabilize TORC1 *in vitro* (39). Our work suggests that 4EBP1 may have as yet unrecognized actions that affect mTOR signaling and/or autophagy. Indeed, the effect of 4EBP1 on autophagy was significant, as cell lines with 4EPB1 knockdown displayed increased baseline

levels of autophagy, increased rapamycin induced autophagy, and increased tunicamycin-induced autophagy and the effect of 4EBP1 was abolished in the presence of the autophagy inhibitor bafilomycin A1. The consistency of these findings suggests that 4EBP1 may interact with specific proteins involved in autophagy; the subsequent discovery of how 4EBP1 affects autophagy has the potential to provide new insight as to the role of 4EBP1 in cellular physiology and cancer.

Our discoveries of the significant effect of MYC on rapamycin, the effect of MYC on 4EBP1 expression, and the effect of 4EBP1 on autophagy suggest that these proteins and the process of autophagy are important to the response of prostate tumor to mTOR inhibition. However, the results from established prostate cancer cell lines and 4EBP1 knockdown experiments suggest that the effect of MYC on rapamycin sensitivity is not entirely explained by the increased expression of 4EBP1 and/or the modulation of autophagy. It is likely that MYC has additional roles that affect a cell's sensitivity to mTOR inhibition and we did note modest increase in pAKT with increased MYC expression, suggesting that TORC2 activity may also be affected. Fortunately, using a recently described dual PI3K and mTOR inhibitor, the effect of MYC on sensitivity is eliminated. Coincidently, BEZ235 dramatically reduces p4EBP and pAKT and increases autophagy and may prove to be a more effective, MYC-independent therapeutic strategy in advanced prostate cancer.

Our work provides a specific example of how confounding genetic events can affect the efficacy of a targeted therapy. As comprehensive genomic analyses for each of the major tumor types become available, work such as that presented in this article will provide a means to understanding how the co-occurrence of specific genetic events may affect a patient's response to a given targeted therapy. The use of genetically engineered cells can help identify specific modulating genetic events that are important to consider when choosing therapy for individuals with cancer. Our results suggest that the limited clinical efficacy of mTOR inhibition in prostate

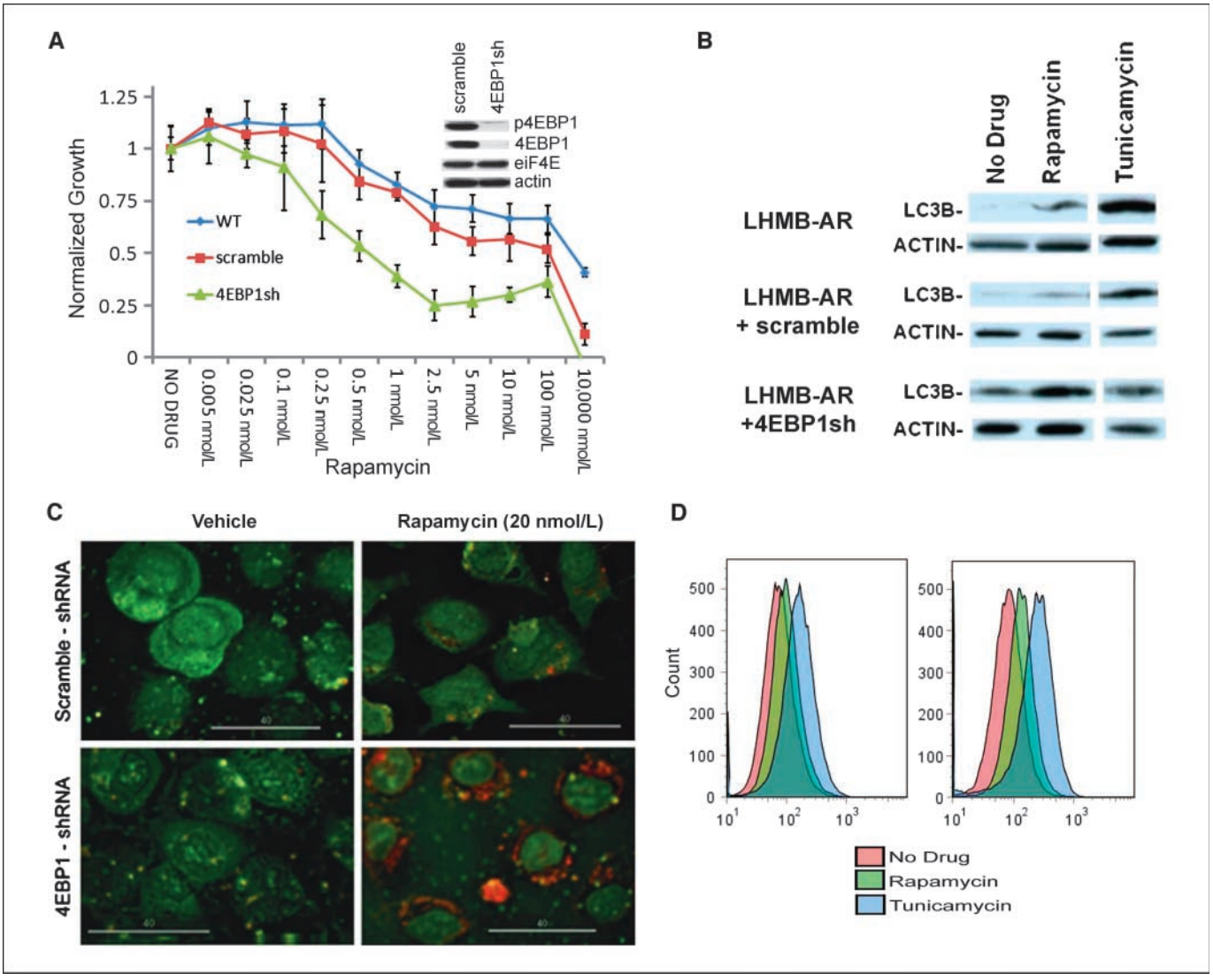

Figure 5. Decreased 4EBP1 leads to increased sensitivity to rapamycin and increased autophagy. *A,* shRNA suppression of 4EBP1 increases sensitivity to rapamycin. Relative cell number at 4 d for each cell line is normalized to culture in the absence of rapamycin and plotted against increasing rapamycin concentration. *B,* decreasing 4EBP1 increases autophagy. Western blot for LC3B following 24 h exposure to 1 μmol/L rapamycin or 2.5 μmol/L tunicamycin. *C,* accumulation of autophagosomes (*red*) during autophagy. *Bar,* 40 μm. *D,* autophagy analyzed using flow cytometry. Cells grown in the presence of 20 nmol/L rapamycin, 2.5 μmol/L tunicamycin, or no drug for 48 h were stained with acridine orange. Each treated group for either cell line is statistically different from the untreated group ($P < 0.0001$, Mann-Whitney test).

cancer may be partially attributed to the frequent genetic gain of MYC, increased expression of 4EBP, and decreased autophagy.

Disclosure of Potential Conflicts of Interest

No potential conflicts of interest were disclosed.

Acknowledgments

Received 3/9/09; revised 7/14/09; accepted 7/28/09; published OnlineFirst 9/22/09.

Grant support: National Cancer Institute grant 123175 and Prostate Cancer Foundation. P.G. Febbo is a Damon Runyon-Lily Clinical Investigator.

The costs of publication of this article were defrayed in part by the payment of page charges. This article must therefore be hereby marked *advertisement* in accordance with 18 U.S.C. Section 1734 solely to indicate this fact.

References

1. Majumder PK, Febbo PG, Bikoff R, et al. mTOR inhibition reverses Akt-dependent prostate intraepithelial neoplasia through regulation of apoptotic and HIF-1-dependent pathways. Nat Med 2004;10:594–601.

2. Podsypanina K, Lee RT, Politis C, et al. An inhibitor of mTOR reduces neoplasia and normalizes p70/S6 kinase activity in Pten$^{+/-}$ mice. Proc Natl Acad Sci U S A 2001; 98:10320–5.

3. Sarbassov dos D, Ali SM, Sabatini DM. Growing roles for the mTOR pathway. Curr Opin Cell Biol 2005; 17:596–603.

4. Hara K, Yonezawa K, Weng QP, Kozlowski MT, Belham C, Avruch J. Amino acid sufficiency and mTOR regulate p70 S6 kinase and eIF-4E BP1 through a common effector mechanism. J Biol Chem 1998;273:14484–94.

5. Xu G, Kwon G, Cruz WS, Marshall CA, McDaniel ML. Metabolic regulation by leucine of translation initiation through the mTOR-signaling pathway by pancreatic β-cells. Diabetes 2001;50:353–60.

6. Dennis PB, Jaeschke A, Saitoh M, Fowler B, Kozma SC, Thomas G. Mammalian TOR: a homeostatic ATP sensor. Science 2001;294:1102–5.

7. Kim DH, Sarbassov DD, Ali SM, et al. mTOR interacts with raptor to form a nutrient-sensitive complex that signals to the cell growth machinery. Cell 2002;110: 163–75.

8. Hara K, Maruki Y, Long X, et al. Raptor, a binding partner of target of rapamycin (TOR), mediates TOR action. Cell 2002;110:177–89.

9. Kim DH, Sarbassov DD, Ali SM, et al. GβL, a positive regulator of the rapamycin-sensitive pathway required for the nutrient-sensitive interaction between raptor and mTOR. Mol Cell 2003;11:895–904.

10. Hashemolhosseini S, Nagamine Y, Morley SJ, Desrivieres S, Mercep L, Ferrari S. Rapamycin inhibition of the G_1 to S transition is mediated by effects on cyclin D1 mRNA and protein stability. J Biol Chem 1998;273: 14424–9.

11. West MJ, Stoneley M, Willis AE. Translational induction of the c-myc oncogene via activation of the FRAP/TOR signalling pathway. Oncogene 1998;17: 769–80.

12. Jefferies HB, Reinhard C, Kozma SC, Thomas G. Rapamycin selectively represses translation of the "polypyrimidine tract" mRNA family. Proc Natl Acad Sci U S A 1994;91:4441–5.

13. Jefferies HB, Fumagalli S, Dennis PB, Reinhard C, Pearson RB, Thomas G. Rapamycin suppresses 5′TOP mRNA translation through inhibition of p70S6K. EMBO J 1997;16:3693–704.

14. Sarbassov DD, Ali SM, Kim DH, et al. Rictor, a novel binding partner of mTOR, defines a rapamycin-insensitive and raptor-independent pathway that regulates the cytoskeleton. Curr Biol 2004;14:1296–302.

15. Jacinto E, Loewith R, Schmidt A, et al. Mammalian TOR complex 2 controls the actin cytoskeleton and is rapamycin insensitive. Nat Cell Biol 2004;6:1122–8.

16. Berger R, Febbo PG, Majumder PK, et al. Androgen-induced differentiation and tumorigenicity of human prostate epithelial cells. Cancer Res 2004;64:8867–75.

17. Febbo PG, Lowenberg M, Thorner AR, Brown M, Loda M, Golub TR. Androgen mediated regulation and functional implications of fkbp51 expression in prostate cancer. J Urol 2005;173:1772–7.

18. Boehm JS, Hession MT, Bulmer SE, Hahn WC. Transformation of human and murine fibroblasts without viral oncoproteins. Mol Cell Biol 2005;25: 6464–74.

19. Leung JY, Ehmann GL, Giangrande PH, Nevins JR. A role for Myc in facilitating transcription activation by E2F1. Oncogene 2008;27:4172–9.

20. Skehan P. Cytotoxicity and cell growth assays. In: Celis JE, editor. Cell biology: a laboratory handbook. 2nd ed. San Diego: Academic Press; 1998. p. 313–8.

21. Singh D, Febbo PG, Ross K, et al. Gene expression correlates of clinical prostate cancer behavior. Cancer Cell 2002;1:203–9.

22. Bolstad BM, Irizarry RA, Astrand M, Speed TP. A comparison of normalization methods for high density oligonucleotide array data based on variance and bias. Bioinformatics 2003;19:185–93.

23. Irizarry RA, Bolstad BM, Collin F, Cope LM, Hobbs B, Speed TP. Summaries of Affymetrix GeneChip probe level data. Nucleic Acids Res 2003;31:e15.

24. Reiter RE, Sato I, Thomas G, et al. Coamplification of prostate stem cell antigen (PSCA) and MYC in locally advanced prostate cancer. Genes Chromosomes Cancer 2000;27:95–103.

25. Current protocols in molecular biology. John Wiley and sons; 2005. p. 21.3.1–33.

26. Neshat MS, Mellinghoff IK, Tran C, et al. Enhanced sensitivity of PTEN-deficient tumors to inhibition of FRAP/mTOR. Proc Natl Acad Sci U S A 2001;98:10314–9.

27. Stone K, Mickey D, Wunderli H, Mickey G, Paulson D. Isolation of a human prostate carcinoma cell line (DU 145). Int J Cancer 1978;21:274–81.

28. Kaighn M, Narayan K, Ohnuki Y, Lechner J, Jones L. Establishment and characterization of a human prostate carcinoma cell line (PC-3). Invest Urol 1979;17:16–23.

29. Horoszewicz JS, Leong SS, Kawinski E, et al. LNCaP model of human prostatic carcinoma. Cancer Res 1983; 43:1809–18.

30. Cao C, Subhawong T, Albert JM, et al. Inhibition of mammalian target of rapamycin or apoptotic pathway induces autophagy and radiosensitizes PTEN null prostate cancer cells. Cancer Res 2006;66:10040–7.

31. Bello-Fernandez C, Packham G, Cleveland JL. The ornithine decarboxylase gene is a transcriptional target of c-Myc. Proc Natl Acad Sci U S A 1993;90:7804–8.

32. Sjoblom T, Jones S, Wood LD, et al. The consensus coding sequences of human breast and colorectal cancers. Science 2006;314:268–74.

33. Jones S, Zhang X, Parsons DW, et al. Core signaling pathways in human pancreatic cancers revealed by global genomic analyses. Science 2008;321:1801–6.

34. McLendon R, Friedman A, Bigner D, et al. Comprehensive genomic characterization defines human glioblastoma genes and core pathways. Nature 2008;455:1061–8.

35. Jenkins RB, Qian J, Lieber MM, Bostwick DG. Detection of c-myc oncogene amplification and chromosomal anomalies in metastatic prostatic carcinoma by fluorescence *in situ* hybridization. Cancer Res 1997;57:524–31.

36. Nupponen NN, Kakkola L, Koivisto P, Visakorpi T. Genetic alterations in hormone-refractory recurrent prostate carcinomas. Am J Pathol 1998;153:141–8.

37. Mark HF, Samy M, Santoro K, Mark S, Feldman D. Fluorescent *in situ* hybridization study of c-myc oncogene copy number in prostate cancer. Exp Mol Pathol 2000;68:65–9.

38. Richter JD, Sonenberg N. Regulation of cap-dependent translation by eIF4E inhibitory proteins. Nature 2005;433:477–80.

39. Wang L, Rhodes CJ, Lawrence JC, Jr. Activation of mammalian target of rapamycin (mTOR) by insulin is associated with stimulation of 4EBP1 binding to dimeric mTOR complex 1. J Biol Chem 2006;281:24293–303.